Urban Water Journal
Publication details, including instructions for authors and subscription information:
http://www.tandfonline.com/loi/nurw20

Pipe hydraulic resistance correction in WDN analysis

O. Giustolisi [a] & E. Todini [b]

[a] Department of Civil and Environmental Engineering, Engineering Faculty of Taranto , Technical University of Bari , via Turismo, 8, Taranto, Italy

[b] Department of Earth and Geo-Environmental Sciences , University of Bologna , Via Zamboni, 67, Bologna, Italy

Published online: 07 Apr 2009.

To cite this article: O. Giustolisi & E. Todini (2009) Pipe hydraulic resistance correction in WDN analysis, Urban Water Journal, 6:1, 39-52, DOI: 10.1080/15730620802541623

To link to this article: http://dx.doi.org/10.1080/15730620802541623

Urban Water Journal
Vol. 6, No. 1, March 2009, 39–52

Taylor & Francis
Taylor & Francis Group

Pipe hydraulic resistance correction in WDN analysis

O. Giustolisi[a]* and E. Todini[b]

[a]*Department of Civil and Environmental Engineering, Engineering Faculty of Taranto, Technical University of Bari, via Turismo, 8, Taranto, Italy;* [b]*Department of Earth and Geo-Environmental Sciences, University of Bologna, Via Zamboni, 67, Bologna, Italy*

(*Received 4 April 2008; final version received 6 August 2008*)

The analysis of a looped water distribution network, operating under pressure and in steady flow conditions, can be accomplished once the topology of the network, the geometry of the pipes, the water demands at the nodes and the head value of at least one node are known. In a water distribution network (WDN), water demands are assigned to the nodes, although in reality they are distributed along the pipes converging at such nodes. This classic assumption represents the total demand along a pipe as two lumped withdrawals at its terminal nodes. This paper demonstrates that the above approximation is wrong because it generates head loss errors which may be significant when network analysis is performed for calibration, system design, real-time operations, rehabilitation strategies, optimal operation studies, reliability analyses, etc. Therefore, an extension of the global gradient algorithm (GGA) for network analysis is proposed which entails a modified GGA permitting the effective introduction of the lumped nodal demands, and without forfeiting a correct physical representation of head losses, by means of a pipe hydraulic resistance correction.

Keywords: hydraulics; network analysis; water distribution modelling

Introduction

The search for the most efficient network simulation algorithm in terms of rapid convergence and robustness (reduced number of cases in which the search for the solution fails) spans a period extending from the application of local linearisation methods in the 1930s (Cross 1936) right down to the end of the 1980s with the development of global linearisation techniques. Global linearisation techniques are characterised by the simultaneous solution of all the equations of the network analysis problem, and the most comprehensive approach to this was set out by Collins *et al.* (1978), who defined the 'content' and 'co-content' models. The 'content' and 'co-content' models are functional in terms of discharge through pipes and nodal head values, respectively, with the 'co-content' model being the dual of the 'content'. Thus, the network analysis problem is reduced to a search for the minimum of the functional (either in terms of pipe discharge or nodal head), which is performed by means of numerical gradient techniques such as those proposed by Collins *et al.* (1978) and Contro and Franzetti (1983).

Alternatively, Todini (1979) and Todini and Pilati (1988) solved the system of equations in terms of the discharge and head values. This second way of addressing the problem is in effect much more traditional since, historically, the study of water supply networks proceeded directly from the setting of the equations for mass conservation at the nodes and energy conservation along the pipes of the network. The Todini and Pilati (1988) solution is thus linear and partly non-linear, producing unknown pipe discharges and nodal head values, respectively. Nonetheless, given the convexity of the content functional, which guarantees the existence and the uniqueness of the solution (Collins *et al.* 1978), linearisation of the non-linear equations can be performed efficiently by means of Newton-Raphson gradient techniques. Then, the mathematical problem is reduced to the iterative solution of a linear system. Accordingly, various algorithms differing from each other in terms of the unknowns used in the differentiation of the original system have been developed. Four different categories of such algorithms are treated in the literature. They can be characterised according to the selected unknowns (Todini 1999):

- All the pipe discharges and all the head values at the nodes giving rise to the algorithm, which is referred to as the Newton-Raphson global

*Corresponding author. Email: o.giustolisi@poliba.it

ISSN 1573-062X print/ISSN 1744-9006 online

DOI: 10.1080/15730620802541623
http://www.informaworld.com

gradient algorithm (Todini 1979, Todini and Pilati 1988). Similar approaches have been described by Hamam and Brameller (1971) and by Carpentier *et al*. (1985) (the 'Hybrid Method') or by Osiadacz (1987) (the 'Newton Loop-Node Method'). The only difference between these approaches and the global gradient lies in the updating of the pipe flows after a new trial solution for nodal heads has been found.

- The pipe discharges causing the head values at the nodes to disappear by means of appropriate linear transformation, giving rise to what is known in the literature as the linear theory algorithm (Wood and Charles 1972, Isaacs and Mills 1980, Wood and Rayes 1981).
- The loop discharge quantities after appropriate linear transformation to re-project the original problem on the closed loops, establishing the algorithm referred to as the Newton-Raphson loop algorithm. This procedure can be seen as an extension of the Cross method, which is local (loop by loop and iterative), to one that is simultaneous (all the loops at the same time) (Epp and Fowler 1970, Kesavan and Chandrashekar 1972).
- The head values at the nodes causing the pipe discharges to disappear by means of appropriate non-linear transformation, producing the Newton-Raphson head algorithm (Martin and Peters 1963, Shamir and Howard 1968, Mignosa 1987).

These algorithms share the common characteristic of requiring the solution of a system of linear equations several times in order to iteratively reach (i.e., by means of successive approximations) the solution of the original system of partly linear and partly non-linear equations. However, the size of the linear system to be solved and the information that has to be provided to formulate it or to identify a first-attempt solution required to initiate the iterative process vary according to the method chosen. Among previous alternatives, the global gradient algorithm (Todini 1979, Todini and Pilati 1988) was found to be the simplest and possibly the most efficient formulation and was used to develop EPANET2 (Rossman 2000), which has probably become the de facto most widely used network simulation model in the world and which is also embedded in several commercial software packages.

Nevertheless, in all the previously discussed and available methods, water demands are uniquely represented as nodal withdrawals, although they are inevitably distributed along the pipes. Therefore, after demonstrating that the above approximation leads to mistaken estimates of the head losses, this article proposes an extension of the global gradient algorithm to allow for a more realistic approximation.

It is worth noting that, although essentially applied to GGA, the standard hydraulic commercial software that relies on other algorithms can also benefit from these improvements. For example, the specific numerical minimisations of the content energy function as proposed by Carpentier *et al*. (1985) and by Piller (1995). In fact, these two algorithms solve the linear system for head and then update the flow rate in a very similar way to that in GGA. The main differences are the Newton direction and step size corrections.

Total head loss of uniformly distributed water demand at pipe level

The assumption of uniformly distributed demands along the pipes is an expedient used when there is poor knowledge about the actual connections and demands. This work will demonstrate how this simple assumption can generate large errors in energy balance conservation when uniform demand is lumped into the two end nodes of a pipe in order to exclusively conserve mass balance. It is worth noting that the results obtained in this classic 'average' assumption are conceptually valid also for different shapes of distributed demands along a pipe (Hamberg and Shamir 1988), considering that in more general cases the error could be higher than that related to the uniform distribution assumption. Furthermore, even when the actual pipe connections and demands are known, coarse simplifications focusing solely on mass balance conservation can produce significant errors in the energy balance, which cannot be corrected without considering the actual network status (i.e., topological and mass balance considerations).

Thus, when uniformly distributed and pressure-independent demands along the pipes are here assumed, the two cases reported in Figure 1a and 1b may occur. The first case (Figure 1a) occurs when $Q_I > P$, where $P = qL$ is the total demand along the pipe. The curve representing the pressure along the pipe is monotonically decreasing and Q_O exits from the pipe, therefore $Q_O \geq 0$ with reference to the assumed positive direction of the longitudinal abscissa x. The second case (Figure 1b) occurs when $P/2 \leq Q_I < P$. Here, the curve representing the pressure has a minimum between the nodes A and B while the direction of Q_O is changed, now being directed towards the pipe, which implies that $Q_O \leq 0$ with reference to the assumed positive direction of the longitudinal abscissa x. It is worth noting that the condition $P/2 \leq Q_I < P$ refers to the assumption, without loss of generality, that $Q_I \geq |Q_O|$ and, for this reason, flow inversion into the pipe occurs at a point x_1 in its second

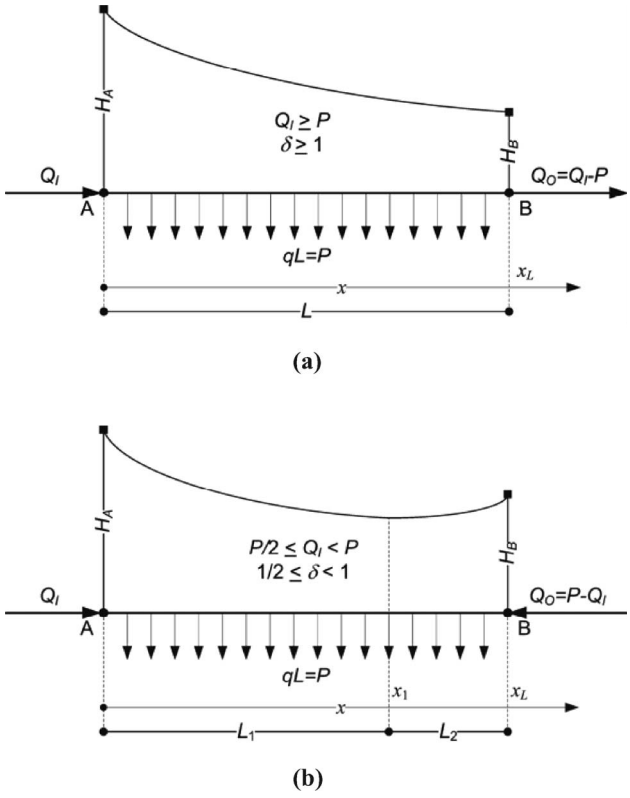

Figure 1. (a) Schematic representation of pipe head without flow inversion. (b) Schematic representation of pipe head with flow inversion.

half. Clearly, for $Q_I = |Q_O| = P/2$ the minimum of the pipe head curve is at the midpoint of the pipe and $H_A - H_B = 0$.

Note that these cases are general and independent of the assumption regarding the shape of the demand distribution along the pipe. In fact, the second case corresponds to all situations involving flow inversion.

The total pipe head loss for the case of Figure 1a can be computed as:

$$H_A - H_B = \int_0^{x_L} K_W(Q_I - qx)|Q_I - qx|^{n-1}dx = \int_0^{x_L} K_W(Q_I - qx)^n dx \quad (1)$$

where K_W is the unitary hydraulic resistance (inverse of the unitary hydraulic conveyance), which is dependent on pipe diameter and material; q is the demand rate uniformly distributed along the pipe; L is the pipe length and x is the longitudinal abscissa. Elimination of the absolute value in Equation (1) is possible because $(Q_I - qx) \geq 0$ for $0 \leq x \leq x_L$. Similarly, for the case of Figure 1*b*, and bearing in mind that $-q(x_1 - x) > 0$ and $qx - Q_I = qx + |Q_O| - P = |Q_O| - q(x_L - x) > 0$, the total pipe head loss can be computed as:

$$\begin{aligned} H_A - H_B &= \int_0^{x_1} K_W(Q_I - qx)|Q_I - qx|^{n-1}dx + \int_{x_1}^{x_L} K_W q(x_1 - x)|q(x_1 - x)|^{n-1}dx \\ &= \int_0^{x_1} K_W(Q_I - qx)^n dx - \int_{x_1}^{x_L} K_W(|Q_O| - q(x_L - x))^n dx \\ &= \int_0^{L_1} K_W(Q_I - qx)^n dx - \int_0^{L_2} K_W(|Q_O| - qy)^n dy \end{aligned} \quad (2)$$

where $y = (x_L - x)$ and $dy = -dx$. The absolute value has been omitted from the first integer because $(Q_I - qx) \geq 0$ for $0 \leq x \leq x_1$. About the second integer $q(x_1 - x) \leq 0$ for $x_1 \leq x \leq x_L$ (that is, the right side of Equation (2)), the minus sign has been introduced. Note that flow inversion occurs when $(Q_I - qx_1) = |Q_O| - q(x_L - x_1)$. Therefore, two lengths, L_1 (corresponding to abscissa x_1) and $L_2 = L - L_1$, can be defined as a function of Q_I, Q_O and q or as a function of a dimensionless quantity δ,

$$L_1 = \frac{Q_I}{q} = \frac{Q_I}{P}L = \delta L$$

and

$$L_2 = L - L_1 = (1 - \delta)$$

$$L = \frac{|Q_O|}{P}L \quad (3)$$

where $\delta = Q_I/P = 1 - |Q_O|/P$.

Integration of Equations (1) and (2) can be easily performed considering the general exponent n. Despite this, and without loss of generality, the assumptions of constant R and $n = 2$ are made here (a particular case of the Darcy-Weisbach head loss formulation), considering that fully turbulent flow is the dominant condition in networks. Nonetheless, extension of the results to alternative equations, such as for instance the widely used Hazen-Williams equation for non-fully turbulent (i.e. $n \neq 2$), is only a mathematical issue.

Thus, integration of Equations (1) and (2), considering that $R = K_W L$, leads to:

$$H_A - H_B = \begin{cases} K_W\left(\frac{Q_I^3 - |Q_O|^3}{3P}\right)L = R\left(\frac{\delta^3 - (1-\delta)^3}{3}\right)P^2 & \frac{1}{2} \leq \delta < 1 \\ K_W\left(Q_I^2 - Q_I P + \frac{P^2}{3}\right)L = R\left(\delta^2 - \delta + \frac{1}{3}\right)P^2 & \delta \geq 1 \end{cases} \quad (4)$$

The important issue is now to find a scheme that can be used in the context of a network simulation model

allowing nodal demands and that abides by mass and energy conservation. Mass conservation constrains the sum of the nodal demands to be equal to $P = qL$ and energy conservation implies that the total pipe head loss must equal $H_A - H_B$ in both cases of Equations (1) and (2) or of Equation (4).

A novel scheme for uniformly distributed demand along the pipe

The classic scheme is to lump αP and $(1-\alpha)P$ in the nodes A and B, respectively. In this way, the total head loss of the pipe is

$$H_A - H_B = K_W(Q_I - \alpha P)^2 L = R(\delta - \alpha)^2 P^2$$

$$\Rightarrow \quad \alpha = \begin{cases} \delta - \sqrt{\frac{2\delta^3 - 3\delta^2 + 3\delta - 1}{3}} & \frac{1}{2} \le \delta < 1 \\ \delta - \sqrt{\delta^2 - \delta + \frac{1}{3}} & \delta \ge 1 \end{cases} \tag{5}$$

and α should be computed as function of δ as reported in Equations (5) and Figure 2.

The drawback of the classic scheme is the absence of the symmetric property with respect to nodal loads and, for this reason, variation of the flow direction into some pipes may decrease convergence of the GGA during iterative search of the solution. Thus, a different scheme is here proposed (Giustolisi and Todini 2008). It is characterised by the symmetric property with respect to nodal loads and the pipe hydraulic resistance (R) is corrected inside the network simulation model in order to account for energy balance conservation. Thus, the first assumption of the scheme is a constant α equal to 0.5, which ensures mass balance conservation and symmetry of the nodal loads with respect to flow direction. Then, the energy balance is obtained by correcting R by means of a term $(1 + \varepsilon)$ in Equation (5). Hence,

$$\begin{cases} R\left(\frac{\delta^3 - (1-\delta)^3}{3}\right) P^2 = (1+\varepsilon) R\left(\delta - \frac{1}{2}\right)^2 P^2 & \\ \quad \Rightarrow \quad \varepsilon = \left(\frac{2}{3}\delta^3 - 2\delta^2 + 2\delta - \frac{7}{12}\right)\left(\delta - \frac{1}{2}\right)^{-2} & \frac{1}{2} \le \delta < 1 \\ R\left(\delta^2 - \delta + \frac{1}{3}\right) P^2 = (1+\varepsilon) R\left(\delta - \frac{1}{2}\right)^2 P^2 & \\ \quad \Rightarrow \quad \varepsilon = \frac{1}{12}\left(\delta - \frac{1}{2}\right)^{-2} & \delta \ge 1 \end{cases} \tag{6}$$

The shape of the function $\varepsilon(\delta)$ is given in Figure 3 for δ bounded in the range [0.6; 2]. Figure 3 clearly shows that the correction ε varies from 0 when $\delta \gg 1$, while it rapidly increases and tends to $+\infty$ when δ approaches 1/2. Thus, the assumption of using $\alpha = 1/2$ without the correction ε may correspond to a vast reduction of the actual pipe head loss due to incorrectness of the energy balance conservation. During calibration, this underestimation of pipe head loss is obviously compensated by using a modified hydraulic resistance $R_{model} = R_{actual}(1 + \varepsilon)$ in the classic approximation scheme, thus inevitably leading to unrealistic hydraulic resistance estimated values. Therefore, hydraulic resistances are generally overestimated and this fact is particularly significant for pipes whose discharges are low with respect to the distributed demand outflow. The overestimation quickly increases for $\delta < 1$. For example, when $\delta = 0.6$, the correction ε is about 4 (see Figure 3). Thus, the calibration of the k-th pipe characterised by a low discharge $[|Q_k| = Q_I - P_k/2 = (\delta - 1/2)P_k]$ becomes unrealistic without considering the correct scheme in the network simulation model.

Clearly then, the two important properties of the proposed scheme are symmetry with respect to nodal demands and the automatic accounting for flow direction, which is embedded into the definition of

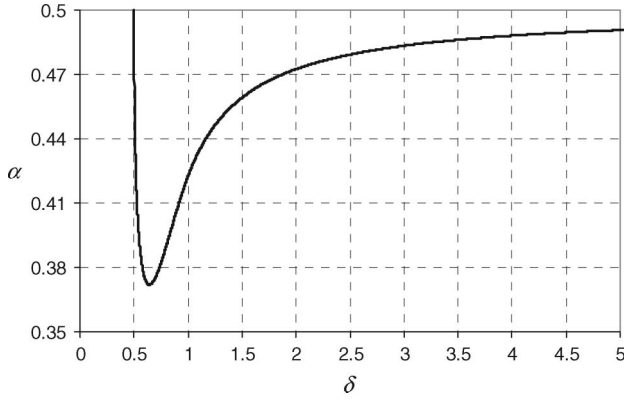

Figure 2. Graphical representation of α as a function of δ.

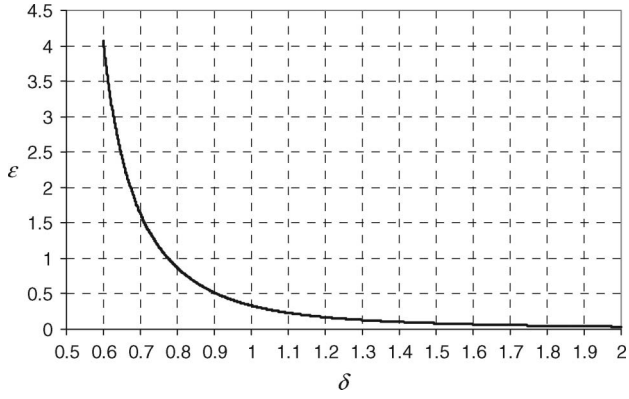

Figure 3. Correction ε on hydraulic resistance as a function of δ.

pipe head losses [$H_A - H_B = R_k|Q_k|Q_k$]. Furthermore, given that the correction is applied to pipe hydraulic resistance, it is easy to implement it into the GGA considering the use of $\alpha = 1/2$ while adding the information on the distributed demand through P_k, as subsequently reported. Finally, it is essential to point out that, although the correction ε tends to $+\infty$ for δ approaching 1/2, this does not affect the terms to be introduced into the GGA, which are always finite.

Error on head losses due to the nodal representation of pipe demand

In order to study the error ($E_{\Delta H}$) on total pipe head loss $H_A - H_B$, it is necessary to write ε of Equation (6) in terms of $|Q_k|$ and P_k relevant to the k-th pipe and to consider the sign of Q_k. The assumption of $\alpha = 1/2$ allows the following expressions,

$$|Q_k| = Q_I - \frac{P_k}{2} \geq 0 \quad \Rightarrow \quad \frac{|Q_k|}{P_k} = \frac{Q_I}{P_k} - \frac{1}{2} \geq 0 \quad \Rightarrow \quad \delta_k = \delta - \frac{1}{2} \geq 0 \quad k = 1, 2, \ldots, n_p \tag{7}$$

where δ_k has the same meaning of δ, but is computed using the state variable Q_k of the network simulation model. Thus, by substituting the results of Equation (7) into Equation (6), it is possible to obtain the pipe hydraulic resistance correction, namely ε_k, as function of the k-th pipe flow rate and uniformly distributed demand:

$$\varepsilon_k = \begin{cases} \left(\frac{2}{3}\delta_k^3 - \delta_k^2 + \frac{1}{2}\delta_k\right)\delta_k^{-2} & 0 \leq \delta_k < \frac{1}{2} \\ \frac{1}{12}\delta_k^{-2} & \delta_k \geq \frac{1}{2} \end{cases} \tag{8}$$

Using ε_k it is now possible to derive the expression for $E_{\Delta H}$,

$$E_{\Delta H} = \varepsilon_k R_k Q_k |Q_k| = \begin{cases} R_k P_k^2 \left(\frac{2}{3}\delta_k^3 - \delta_k^2 + \frac{1}{2}\delta_k\right) sign(Q_k) & 0 \leq \delta_k < \frac{1}{2} \\ R_k \frac{P_k^2}{12} sign(Q_k) & \delta_k \geq \frac{1}{2} \end{cases} \tag{9}$$

Equation (9) can also be rewritten as function of R_k, P_k and the dimensionless parameter z_k, in order to be used in WDN simulation models:

$$E_{\Delta H} = z_k R_k P_k^2 sign(Q_k) \quad \text{where } z_k = \begin{cases} \left(\frac{2}{3}\delta_k^3 - \delta_k^2 + \frac{1}{2}\delta_k\right) & 0 \leq \delta_k < \frac{1}{2} \\ \frac{1}{12} & \delta_k \geq \frac{1}{2} \end{cases} \tag{10}$$

It is important to note that the correction of pipe head losses defined in Equation (10) always tends to increase the absolute value of ΔH. Furthermore, the flow direction is now incorporated into the expression of $E_{\Delta H}$ through the function sign(Q_k), which means that there is no need to change the nodal demand as a function of the flow direction, as expected using $\alpha = 1/2$.

Furthermore, assuming $P_k = 1\ \mathrm{m^3 s^{-1}}$ and $R_k = 1\ \mathrm{s^2\ m^{-5}}$, and considering that $z_k \geq 0$, $E_{\Delta H}$ can be represented as function of the dimensionless $Q_k/P_k = \delta_k\ \mathrm{sign}(Q_k)$ value as graphically shown in Figure 4. As one can see from the figure, the derivative of $E_{\Delta H}$ with respect to Q_k is always positive, as it is for $R_k|Q_k|Q_k$, the basic term expressing the head losses. This can be shown from Equation (11):

$$H_A - H_B = R_k\left(Q_k^2 + z_k P_k^2\right) sign(Q_k) \tag{11}$$

which better explains the fact that the derivative of the corrected total head loss is always positive given that both terms in the round brackets are non negative. This is an important issue when computing the derivatives in the GGA algorithm.

Enhanced GGA network simulation model

The demand-driven simulation of a network of n_p pipes with unknown discharges, n_n nodes with unknown heads (internal nodes) and n_0 nodes with known heads (tank levels, for example) can be described in matrix form as in Todini and Pilati (1988). Therefore, assuming the elements of the diagonal matrix $\mathbf{A}_{pp}$ of order n_p equal to $R_k|Q_k|^{n-1}$, the demand-driven simulation of a network is formulated in the following non-linear system of equations based on energy and mass balance conservations

$$\begin{bmatrix} \mathbf{A}_{pp} & \mathbf{A}_{pn} \\ \mathbf{A}_{np} & \mathbf{0} \end{bmatrix} \begin{bmatrix} \mathbf{Q} \\ \mathbf{H} \end{bmatrix} = \begin{bmatrix} -\mathbf{A}_{p0}\mathbf{H}_0 \\ \mathbf{d} \end{bmatrix} \tag{12}$$

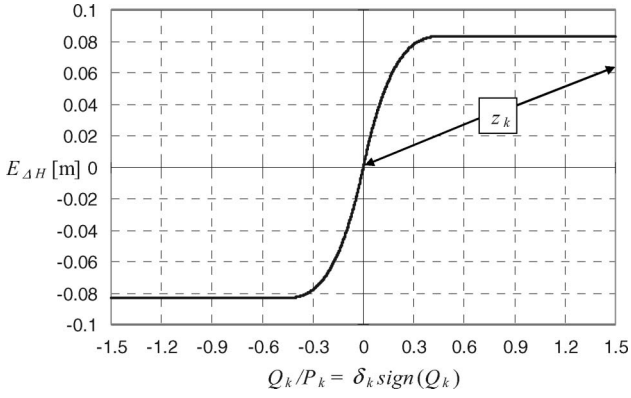

Figure 4. Graphical representation of $E_{\Delta H}$ given by Equation (10) as a function of Q_k.

where $\mathbf{Q}$ is the $[n_p,1]$ column vector of unknown pipe flow rates, $\mathbf{H}$ is the $[n_n,1]$ column vector of unknown nodal heads, $\mathbf{H}_0$ is the $[n_0,1]$ column vector of known nodal heads, $\mathbf{A}_{pn} = \mathbf{A}^T{}_{np}$ and $\mathbf{A}_{p0}$ are topological incidence sub-matrices of size $[n_p, n_n]$ and $[n_p, n_0]$, respectively, derived from the general topological matrix $\bar{\mathbf{A}}_{pn} = [\mathbf{A}_{pn} \mid \mathbf{A}_{p0}]$ of size $[n_p, n_n + n_0]$, as defined in Todini and Pilati (1988). The solution of the non-linear system in Equation (12) using the GGA was originally proposed by Todini (1979). Successively, the demand-driven case was expanded, for example, by Todini (2003) and Giustolisi *et al.* (2008a,b), to account for pressure-driven demands and leakage. In this paper, Equation (13) summarises the demand-driven case at the i-th iteration:

$$\begin{aligned}
\mathbf{A}^i &= \mathbf{A}_{np}\left(\mathbf{D}^i_{pp}\right)^{-1}\mathbf{A}_{pn}\\
\mathbf{F}^i &= \left(\mathbf{A}_{np}\mathbf{Q}^i - \mathbf{d}\right) - \mathbf{A}_{np}\left(\mathbf{D}^i_{pp}\right)^{-1}\left(\mathbf{A}^i_{pp}\mathbf{Q}^i + \mathbf{A}_{p0}\mathbf{H}_0\right)\\
\mathbf{H}^{i+1} &= \left(\mathbf{A}^i\right)^{-1}\mathbf{F}^i\\
\mathbf{Q}^{i+1} &= \mathbf{Q}^i - \left(\mathbf{D}^i_{pp}\right)^{-1}\left(\mathbf{A}^i_{pp}\mathbf{Q}^i + \mathbf{A}_{p0}\mathbf{H}_0 + \mathbf{A}_{pn}\mathbf{H}^{i+1}\right)
\end{aligned} \tag{13}$$

Starting from Equation (11), it is possible to derive a corrected expression for the diagonal matrix $\mathbf{D}_{pp}$ to be used in Equation (13). Hence,

$$\begin{aligned}
D_{pp}(k,k) &= \frac{d\left[\left(Q_k^2 + z_k P_k^2\right) sign(Q_k) R_k\right]}{dQ_k}\\
&= (2|Q_k| + z_D P_k) R_k
\end{aligned} \tag{14}$$

where

$$z_D = \frac{P_k}{sign(Q_k)}\frac{dz_k}{dQ_k} = \frac{dz_k}{d\delta_k} = \begin{cases} 2\delta_k^2 - 2\delta_k + \frac{1}{2} & 0 \le \delta_k < \frac{1}{2} \\ 0 & \delta_k \ge \frac{1}{2} \end{cases} \tag{15}$$

From Equation (14), one appreciates that $\mathbf{D}_{pp}$ is a positive function. Its classic dependency on R_k and $|Q_k|$ is now completed by P_k and the dimensionless parameter z_D. Figure 5 shows that z_D decreases from the value 1/2 when $\delta_k = 0$ to 0 when $\delta_k = 1/2$.

As with the correction for $\mathbf{D}_{pp}$, and starting from Equation (11), it is possible to derive a corrected expression for the diagonal matrix $\mathbf{A}_{pp}$ to be used in Equation (13). Hence,

$$\begin{aligned}
A_{pp}(k,k) &= \frac{\left[\left(Q_k^2 + z_k P_k^2\right) sign(Q_k) R_k\right]}{Q_k}\\
&= \left(|Q_k| + z_k \frac{P_k^2}{|Q_k|}\right) R_k = (|Q_k| + z_A P_k) R_k
\end{aligned} \tag{16}$$

where

$$z_A = \frac{z_k}{\delta_k} = \begin{cases} \frac{2}{3}\delta_k^2 - \delta_k + \frac{1}{2} & 0 \le \delta_k < \frac{1}{2} \\ \frac{1}{12\delta_k} & \delta_k \ge \frac{1}{2} \end{cases} \tag{17}$$

Note that from Equation (16) it is possible to discern that $\mathbf{A}_{pp}$ is a positive function. Its classic dependency on R_k and $|Q_k|$ is also now completed by P_k and the dimensionless parameter z_A. Figure 6 reveals that z_A decreases from the value 1/2 when $\delta_k = 0$ to 0 when δ_k tends to ∞.

Finally, considering the GGA in Equation (13), it may be useful to compute the diagonal element of the product $\mathbf{A}_{pp}(\mathbf{D}_{pp})^{-1}$. Again, starting from Equations (14) and (16), it is possible to obtain:

$$\frac{A_{pp}(k,k)}{D_{pp}(k,k)} = \frac{|Q_k| + z_A P_k}{2|Q_k| + z_D P_k} = \frac{\delta_k + z_A}{2\delta_k + z_D} = z_{AD} \tag{18}$$

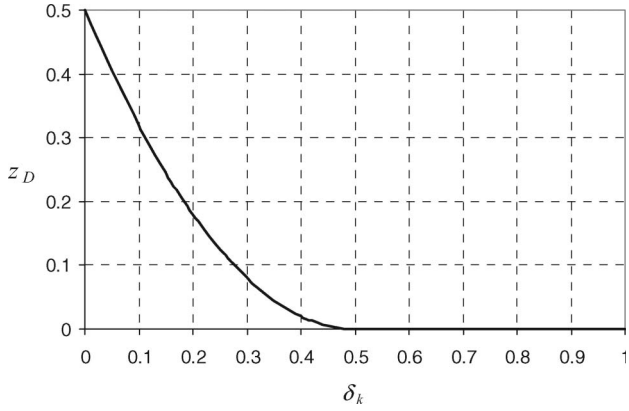

Figure 5. Graphical representation of z_D given by Equation (15) as a function of δ_k.

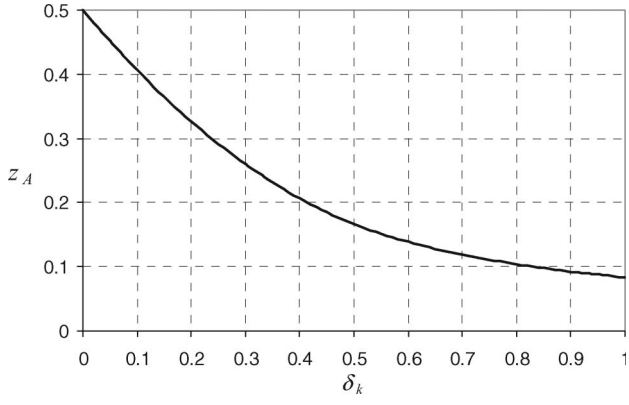

Figure 6. Graphical representation of z_A given by Equation (17) as a function of δ_k.

where

$$z_{AD} = \frac{\delta_k + z_A}{2\delta_k + z_D} = \begin{cases} \frac{4\delta_k^2+3}{12\delta_k^2+3} & 0 \le \delta_k < \frac{1}{2} \\ \frac{1}{2}\left(1 + \frac{1}{12\delta_k^2}\right) & \delta_k \ge \frac{1}{2} \end{cases} \quad (19)$$

From Equation (18), the product $\mathbf{A}_{pp}(\mathbf{D}_{pp})^{-1}$ can be observed as a positive function of $|Q_k|$ and P_k or of the dimensionless parameter z_{AD}. Figure 7 shows that z_{AD} decreases from the value 1 when $\delta_k = 0$ to 1/2 when δ_k tends to ∞.

Finally, it is worth noting that the classic formulation can be achieved when δ_k tends to ∞ corresponding to $z_D = 0$, $z_A = 0$ and $z_{AD} = 1/2$ or when $P_k = 0$.

Case study: a simple hydraulic system

The implications for calibration results of the modified GGA, accounting in a more realistic way for uniformly distributed water demands along pipes, are here discussed analysing the simple hydraulic system depicted in Figure 8. The system is composed of two tanks, T1 and T2, whose levels are 30 m and 20 m, respectively. The tanks are connected by means of three 500 m long pipes characterised by the same hydraulic resistance value of $K_w = R_{k=1,2,3}/\mathrm{L} = 265.147\ \mathrm{s^2\ m^{-6}}$. Pipe no. 2 is the only one subject to uniformly distributed water demand. It is assumed to be at most $P_{max} = 0.02\ \mathrm{m^3\ s^{-1}}$ during peak hours. Figure 9 depicts the assumed pattern of hourly demand for the 24-hour extended period simulation (EPS).

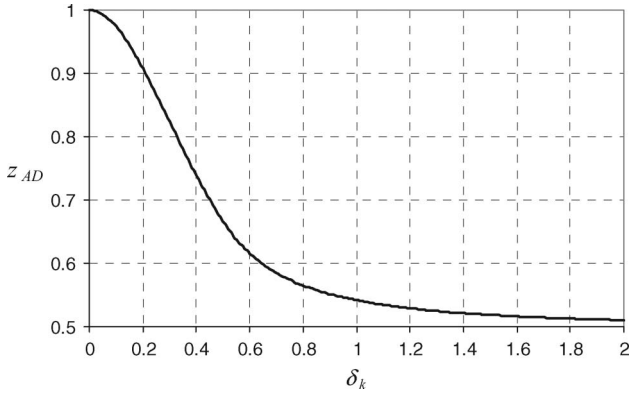

Figure 7. Graphical representation of z_{AD} given by Equation (19) as a function of δ_k.

Using this basic system, comparison between the classical solution (replacing the distributed demand with nodal demand, half of which is distributed at each terminal node without correcting the pipe hydraulic resistance) and the proposed solution (replacing the distributed demand with nodal which is apportioned equally to each node but now correcting the pipe hydraulic resistance) was undertaken.

Discussion of results

In order to cover the loading conditions of Equations (1) and (2), the example of Figure 8 is characterised by two different operating conditions: (i) the tank T1 delivers the water demand requested by pipe no. 2 and fills tank T2 and; (ii) both the tanks T1 and T2 cover the water demand requested by pipe no. 2. Clearly, the first condition occurs during the night hours when the lower demand of pipe no. 2 can be completely delivered by tank T1 considering the 10 m head difference between tank levels.

Figure 10 shows the hydraulic grade lines of the system at different hours ($t = 3$ h, 8 h, 15 h) computed using both the original and the modified GGA. The grade line at time $t = 3$ h is relevant to working condition (i) in which the slopes H(B)–T2 are negative, while the grade lines for $t = 8$ h and $t = 15$ h relate to working condition (ii) in which the slopes H(B)–T2 are positive. In the cases of $t = 3$ h, the night condition, the difference between the grade lines computed with and without GGA modification is much lower than in

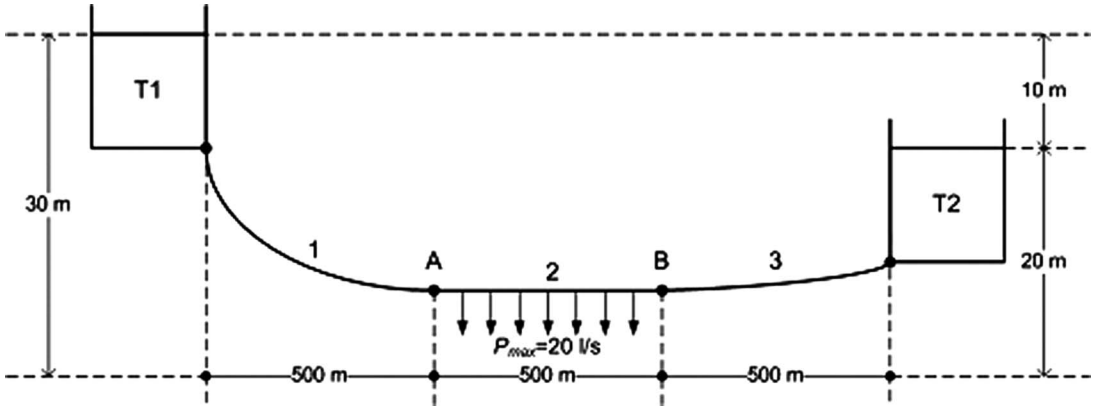

Figure 8. Case study: calibration of pipe hydraulic resistance in EPS mode.

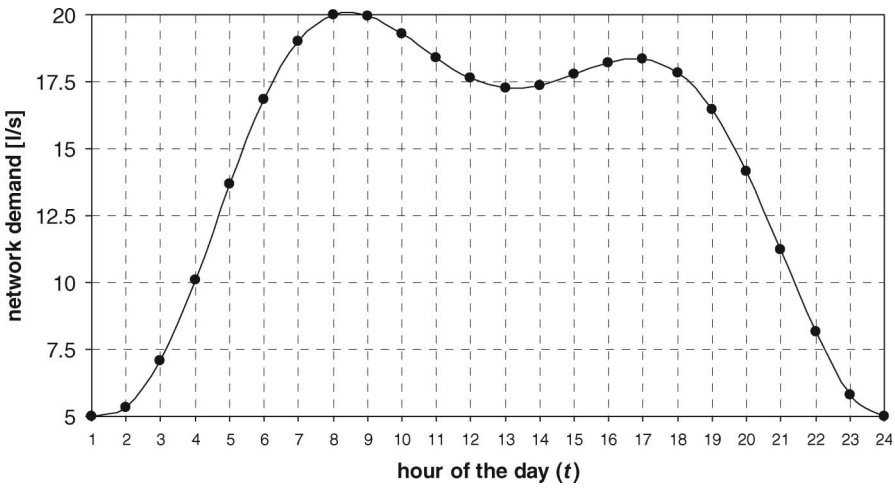

Figure 9. Daily-demand variation $P(t)$.

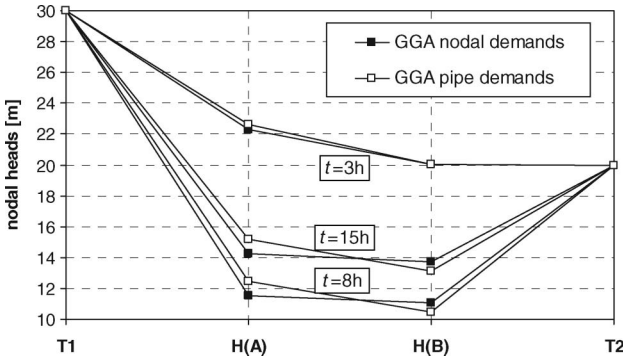

Figure 10. Nodal heads at different hours ($t = 3$ h, 8 h, 15 h). Network analysis using modified or classic GGA.

the cases $t = 8$ h and $t = 15$ h. This can also be noted from Figure 11 where the daily pattern of the total head loss of pipe no. 2 is displayed. It is worth noting that the difference between head losses, $E_{\Delta H}$ previously defined as a function of $R_{k=2}$, $\delta_{k=2}$ and $P_{k=2}$, is at its maximum and remains essentially constant during the middle hours of the day. This is caused by a lower $\delta_{k=2}$ originating from a greater water demand to be supplied by both tanks T1 and T2. This is clear from Figure 12 which shows the daily variation of the $\delta_{k=2}$ value. $\delta_{k=2}$ is larger than 1/2 for $t = 1$ h, 2 h, 3 h, 23 h and 24 h – hydraulic condition (i) – while it is lower during the other hours – hydraulic condition (ii).

It is worthwhile noticing that the hydraulic resistance correction is not constant in time. Using the available data and results it is easy to compute the corrected hydraulic resistance:

$$R_{k=2}^{\text{modified GGA}}(t) = \frac{H_A(t) - H_B(t)}{Q_{k=2}^2(t)} = R_{k=2}^{\text{original GGA}}(1 + \varepsilon_{k=2}(t)) \qquad (20)$$

Equation (20) provides a non unique value of $R_{k=2}$, varying t because of the incorrectness of the model. In fact, Figure 13 exhibits a wide variation of $\varepsilon_{k=2}(t)$ during the day due to fluctuation of $\delta_{k=2}(t)$ (i.e. hydraulic conditions). Considering that the mean value of $\varepsilon_{k=2}$ is roughly equal to 3, Equation (20) will yield an average $R_{k=2}$ which is more or less 'four times greater' $(1 + \varepsilon_{mean})$ than the real value.

An additional experiment was carried out to show the consequences of the reported error on the calibration, namely when one tries to estimate the unknown hydraulic resistance from the assumed demand and observed head patterns. This was done by estimating R_k by means of a multi-objective genetic algorithm (MOGA) (Goldberg 1989) to calibrate the system. Now, the assumption is that $H_A(t)$ and $H_B(t)$ of the system in Figure 8 are known together with the hourly demands of Figure 9, which are concentrated in the nodes A and B (unmodified GGA).

The decision variables used in MOGA are the coefficients $x_{GA}(k = 1{:}3)$ which are multipliers of the hydraulic resistance $R_{k=1:3}$ used for the simulation of the calibrated system. The objective functions to minimise are:

$$\text{err}(H) = \sum_{t=1}^{24} \frac{\left|H_A(t) - H_A^*(t)\right| + \left|H_B(t) - H_B^*(t)\right|}{48} \qquad (21)$$

and the standard deviation (StD) of x_{GA}. In Equation (21), H^* are the nodal heads computed using the calibrated model. The minimisation err(H) is a classic objective and the minimisation of StD(x_{GA}) is useful in order to analyse the effect of pipe grouping. The results of MOGA optimisation are reported in Figure 14. It reveals that x_{GA} related to pipes no. 2 and no. 3 decreases to 1.01, slightly increasing err(H). Thus, the

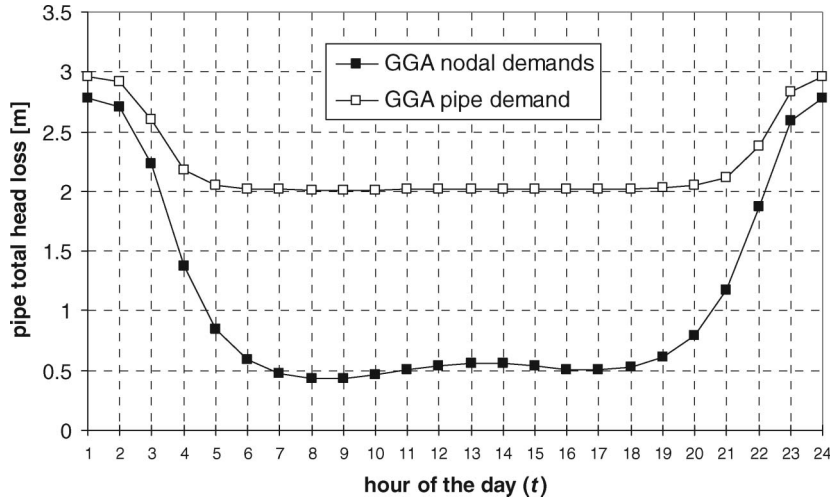

Figure 11. Total head loss of pipe no. 2 at different hours (t). Network analysis using modified or classic GGA.

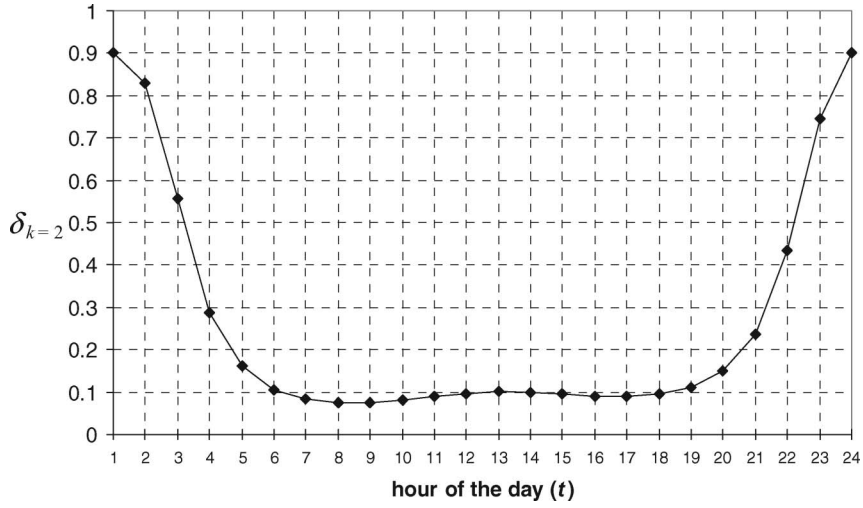

Figure 12. Ratio between pipe discharge and total uniformly distributed demand δ_k for pipe no. 2 at different hours.

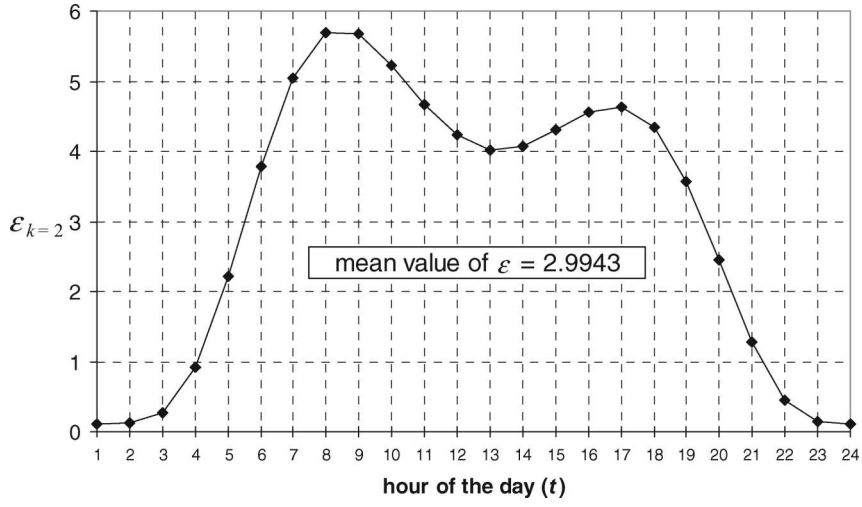

Figure 13. Hydraulic resistance correction ε_k for pipe no. 2 at different hours (t).

solution providing the minimum err(H) (= 0.4424 m) has the maximum StD(x_{GA}) corresponding to $x_{GA}(k = 1{:}3)$ = [1.01, 2.21, 1.07]. This solution corresponds to a system calibration without grouping the pipes. In this circumstance, the correction of pipe no. 2 is high and corrupts the calibration of the whole system even if the pipes no. 1 and 3 do not distribute any demand and, for this reason, do not require the correction ε in the modified GGA being $P_k = 0$.

The solution providing the maximum err(H) (= 0.5636 m) has the minimum StD(x_{GA}) (= 0) corresponding to $x_{GA}(k = 1{:}3)$ = [1.01, 1.01, 1.01]. Thus, the extra information regarding correlation among hydraulic resistances in the system (grouping) renders the calibration error err(H) greater but it simultaneously provides calibrated hydraulic resistance closer to the actual value. Finally, the experiment on the simple system of Figure 8 demonstrates that the modified GGA is mandatory for system calibration and that use of the unmodified GGA causes hydraulic resistance prediction error for all system pipes.

Case study: a looped network fed by one source of water

The aim of the previous case study was to demonstrate by means of a simple hydraulic system (hence easily

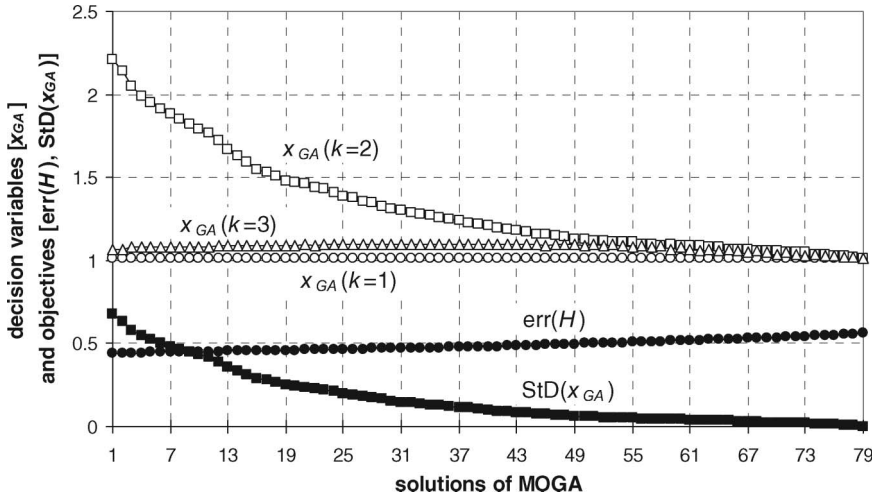

Figure 14. Results of MOGA used for system calibration.

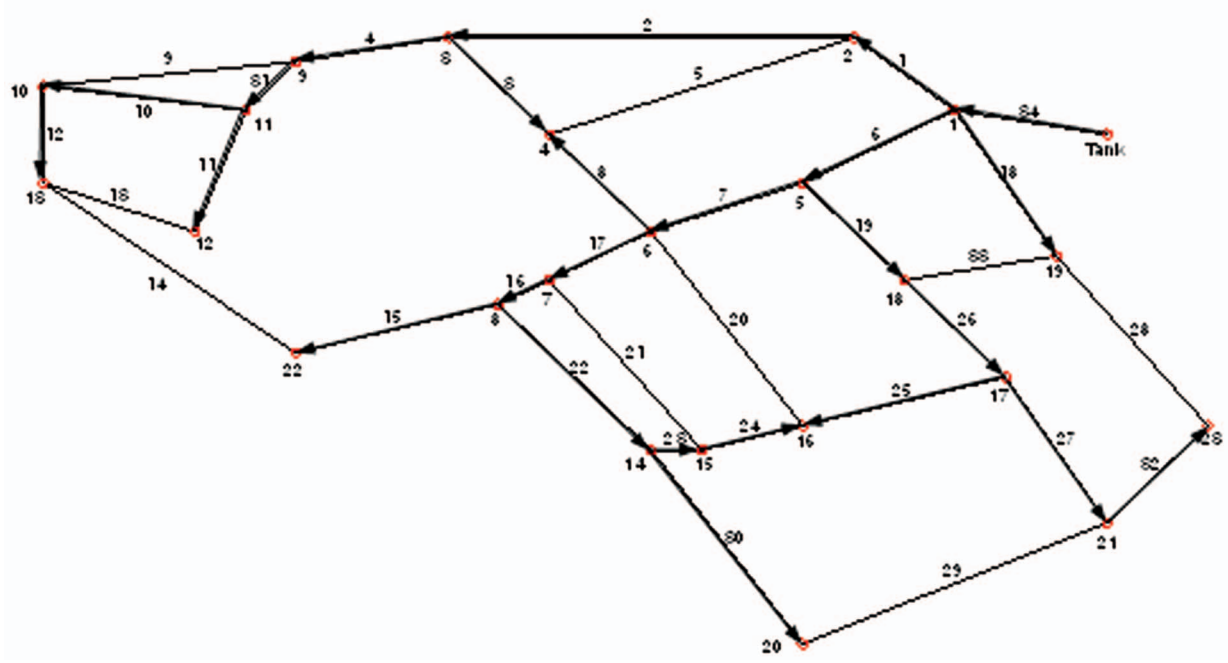

Figure 15. Apulian network layout. The pipes without arrows (flow direction) are characterized by flow inversion.

analysed) the need for a large correction ε to pipe no. 2's hydraulic resistance in order to account for energy balance conservation. In this section, we will address two further questions. Is the approximation of nodal demands without using the pipe hydraulic resistance correction valid in a looped system fed by one source? Is the approximation dependent on demand values or on pipe flow distribution across the network?

Table 1. Apulian network pipe data and node data.

Pipe ID	Length (m)	Diameter (m)	Demand $\mathbf{P}_{design}$ (m^3/s)	Node ID	Elevation (m)
1	348.5	0.327	0.0057	1	6.4
2	955.7	0.290	0.0155	2	7
3	483	0.100	0.0078	3	6
4	400.7	0.290	0.0065	4	8.4
5	791.9	0.100	0.0129	5	7.4
6	404.4	0.368	0.0066	6	9
7	390.6	0.327	0.0063	7	9.1
8	482.3	0.100	0.0078	8	9.5
9	934.4	0.100	0.0152	9	8.4
10	431.3	0.184	0.0070	10	10.5
11	513.1	0.100	0.0083	11	9.6
12	428.4	0.184	0.0070	12	11.7
13	419	0.100	0.0068	13	12.3
14	1023.1	0.100	0.0166	14	10.6
15	455.1	0.164	0.0074	15	10.1
16	182.6	0.290	0.0030	16	9.5
17	221.3	0.290	0.0036	17	10.2
18	583.9	0.164	0.0095	18	9.6
19	452	0.229	0.0073	19	9.1
20	794.7	0.100	0.0129	20	13.9
21	717.7	0.100	0.0117	21	11.1
22	655.6	0.258	0.0107	22	11.4
23	165.5	0.100	0.0027	23	10
24	252.1	0.100	0.0041	24	$H_0 = 36.4$
25	331.5	0.100	0.0054		
26	500	0.204	0.0081		
27	579.9	0.164	0.0094		
28	842.8	0.100	0.0137		
29	792.6	0.100	0.0129		
30	846.3	0.184	0.0138		
31	164	0.258	0.0027		
32	427.9	0.100	0.0070		
33	379.2	0.100	0.0062		
34	158.2	0.368	0		

In order to answer these questions, the Apulian network depicted in Figure 15, whose main data are reported in Table 1 (for further details see Giustolisi *et al.* 2008a), was considered. In particular, Table 1 reports $\mathbf{P}_{design}$, which is the total pipe level demand used for network design (Giustolisi *et al.* 2008b) and is partitioned according to the classical approximation that represents it as two lumped demands at the terminal nodes assuming $\alpha = 1/2$.

The use of a more complicated system fed by one source of water is helpful because the pipe flow rate distribution across the network is driven by the spatial distribution of the pipe demands. Furthermore, the system is not characterised by night and day different working conditions due to the presence of more than one source of water at different head levels as in the previous simple hydraulic system.

Thus, the network in Figure 15 was analysed using modified (pipe hydraulic resistance correction) and unmodified GGA. A pipe level demand vector proportional to $\mathbf{P}_{design}$ was employed and, in particular, Figure 16 reports the nodal pressures of the cases $\mathbf{P} = \mathbf{P}_{design}$ and $\mathbf{P} = 0.75\mathbf{P}_{design}$. Figure 16 confirms that the correction to pipe hydraulic resistance introduces an error to the energy balance also in a looped system, although the two cases ($\mathbf{P} = \mathbf{P}_{design}$ and $\mathbf{P} = 0.75\mathbf{P}_{design}$) demonstrate a rapidly decreasing value of the nodal pressure error (generated by summation along the flow paths of the head loss errors). Clearly, this is a further proof of Equation (10), revealing the dependency on $\mathbf{P}^2$ of the pipe head

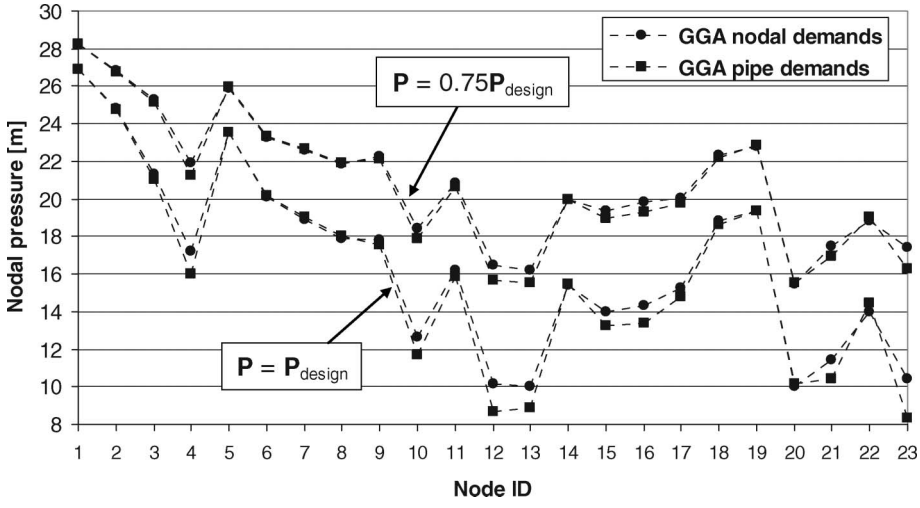

Figure 16. Pressure status of the Apulian network using two demand levels ($\mathbf{P} = \mathbf{P}_{design}$ and $\mathbf{P} = 0.75\mathbf{P}_{design}$).

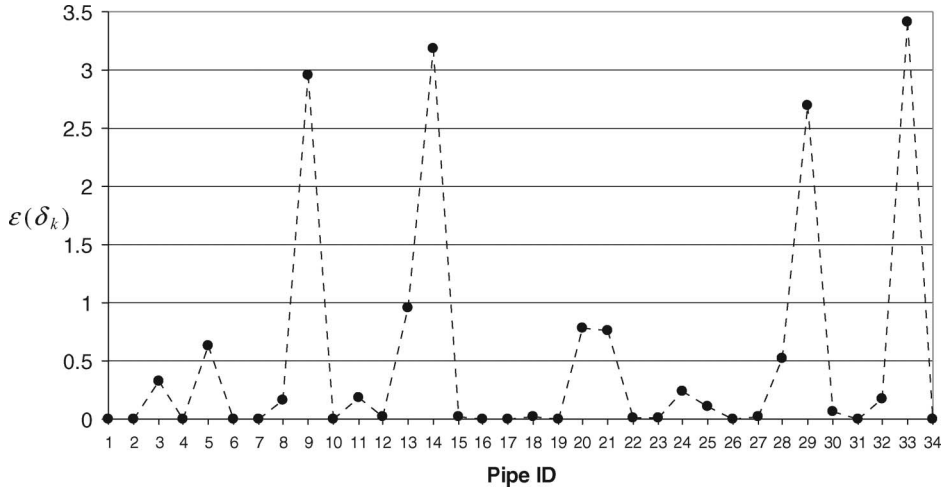

Figure 17. Pipe hydraulic resistance corrections for Apulian network.

loss error. Considering now that the hydraulic resistances of the pipes were constant during analysis of the Apulian network, it is useful to scrutinise ε_k of the k-th pipe varying **P**. Figure 17 reports these values for each pipe ID. Surprisingly, they remain constant with varying **P**, although this result was predictable considering that ε is dependent on δ_k; see Equation (8), which is a dimensionless parameter dependent on the ratio between $|Q_k|$ and P_k. Therefore, the spatial disposition of demands giving rise to the distribution of Q_k drives the values of ε_k across the network. In fact, it was unchanged by the proportional reduction of **P** as for example with the nodes ID (5, 9, 13, 14, 20, 21, 28, 29, 33) characterised by incidents of flow inversion; see Figure 15. This is valid in systems fed by only one water source, as clear from the different behaviour of the simple hydraulic network previously studied. In fact, the presence of more than one source with different head levels generates a different distribution of pipe flows across the network varying **P**. At this point, it is possible to answer the two above questions, affirming that correction of pipe hydraulic resistance is important in all of the systems (looped or not) even if head loss errors are proportional to the second power of **P** (i.e. pipe level qL) and, finally, the pipe hydraulic resistance corrections are driven by pipe flow distribution across the network.

Conclusions

This paper demonstrated that the classical assignation of nodal demands to approximate distributed demands along pipes of a WDN introduces errors in head loss representation that cannot be disregarded since they inevitably lead to poor model calibrations and more generally significant effects on network analysis results.

A simple hydraulic system was useful to prove the need for a large correction to pipe hydraulic resistance in order to account for energy balance conservation. A looped network was helpful to show that the approximation of nodal demands without using the pipe hydraulic resistance correction is not valid in a looped system fed by one source and that the approximation depends on pipe flow distribution across the network and not on demand values.

Therefore, an enhancement of Todini's global gradient algorithm was introduced in order to overcome the problem. The new formulation of the network simulation model can be easily implemented in all simulation packages based on GGA, such as for instance EPANET 2, and it can serve as a guide for other network simulation model strategies. It is envisaged that the new simulation model is essential for network model calibration purposes and also for other network analyses. Finally, it is worthwhile mentioning that the formulation here presented can be easily extended to the general case of non-quadratic head losses.

Notation

The following symbols are used in the paper:

$\mathbf{A}$	= temporary matrix used in simulation model algorithm;
$\bar{\mathbf{A}}_{pn}$	= general topological matrix;
$\mathbf{A}_{pn}$, $\mathbf{A}_{np}$, $\mathbf{A}_{p0}$	= topological incidence sub-matrices;
$\mathbf{A}_{pp}$	= diagonal matrix whose elements are $(\lvert Q_k\rvert + z_A P_k)R_k$;
$\mathbf{d}$	= vector of nodal demands;

$\mathbf{D}_{pp}$ = diagonal matrix whose elements are $(2\,|Q_k| + z_D P_k)R_k$;
$\mathbf{F}$ = temporary matrix used in Todini's algorithm;
$H^*(t)$ = nodal head of the calibrated simulation model at the day-hour t;
$H_A(t)$, $H_B(t)$ = nodal heads (in A and B) of the system in Figure 8 at the day-hour t;
$\mathbf{H}$ = vector of total network heads;
$\mathbf{H}_0$ = vector of total fixed (i.e. known) network heads;
i = counter of the GGA;
k = matrix index for pipes;
K_w = unitary pipe hydraulic resistance, inverse of the unitary hydraulic conveyance;
L = length of pipe;
n = head loss equation exponent and sub-matrix index;
n_0 = total number of known heads;
n_p = total number of network pipes;
n_n = total number of network nodes;
P = total uniformly distributed demand at pipe level;
P_k = total uniformly distributed demand of the k-th pipe;
$\mathbf{P}_{design}$ = pipe level demand used for design purpose in Apulian network;
P_{max}, $P(t)$ = maximum and hourly total uniformly distributed demand in the case study;
q = unitary uniformly distributed demand at pipe level;
Q_I = discharge entering into the pipe;
Q_O = discharge exiting from (no flow inversion) or entering into (flow inversion) the pipe;
$\mathbf{Q}$ = vector of pipe flows;
R_k = pipe hydraulic resistance, inverse of the hydraulic conveyance of the k-th pipe;
z, z_A, z_D, z_{AD} = dimensionless parameters of modified GGA;
α = coefficients used for concentrating the pipe demand into its two ending nodes;
δ = ratio between Q_I and total uniformly distributed demand at pipe level
δ_k = ratio between pipe discharge and total uniformly distributed demand at pipe level;
ε = pipe hydraulic resistance correction;
ε_k = pipe hydraulic resistance correction of k-th pipe in GGA;
x = abscissa used in Figure 1a and 1b;
x_1 = abscissa of flow inversion;
x_L = abscissa of the node B;
x_{GA} = decision variables of MOGA used for simulation model calibration.

Operators and acronyms

EPS = extended period simulation;
GGA = global gradient algorithm;
MOGA = multi-objective genetic algorithm;
sign() = variable sign operator;
WDN = water distribution network;
$()^T$ = vector/matrix transpose operator;
$()^{-1}$ = matrix inverse operator.

References

Carpentier, P., Cohen, G., and Hamam, Y., 1985. Water network equilibrium, variational formulation and comparison of numerical algorithms. EURO VII, Bologna, Italy.

Collins, M., Cooper, L., Helgason, R., Kenningston, J., and LeBlanc, L., 1978. Solving the pipe network analysis problem using optimization techniques. *Management Science*, 24 (7), 747–760.

Contro, R. and Franzetti, S., 1983. A new objective function for analysing hydraulic pipe networks in the presence of different states of flow. *Meccanica*, 18 (4), 225–228.

Cross, H., 1936. *Analysis of flow in networks of conduits or conductors*. Bulletin no. 286, University of Illinois Engineering Experimental Station, Urbana, IL, USA, 1–29.

Epp, R. and Fowler, A.G., 1970. Efficient code for steady-state flows in networks. *Journal of Hydraulic Division, ASCE*, 96 (11), 3–56.

Giustolisi, O., Kapelan, Z., and Savic, D.A., 2008a. An algorithm for automatic detection of topological changes in water distribution networks. *Journal of Hydraulic Engineering, ASCE*, 134 (4), 435–446.

Giustolisi, O., Savic, D.A., and Kapelan, Z., 2008b. Pressure-driven demand and leakage simulation for water distribution networks. *Journal of Hydraulic Engineering, ASCE*, 134 (5), 626–635.

Giustolisi, O. and Todini, E., 2008. On the approximation of distributed demands as nodal demands in WDN analysis. *In*: *Proc. XXXI National Hydraulics and Hydraulic Construction Conference*, 9–12 September, Perugia, Italy.

Goldberg, D.E., 1989. *Genetic algorithms in search, optimization and machine learning*. Addison Wesley.

Hamam, Y.M. and Brammeler, A., 1971. Hybrid method for the solution of piping networks. *Proceedings IEE*, 118 (11), 1607–1612.

Hamberg, D. and Shamir, U., 1988. Schematic Models for Distribution Systems Design: I Combination Concept. *Journal of Water Resources Planning and Management, ASCE*, 114 (2), 129–140.

Kesavan, H.K. and Chandrashekar, M., 1972. Graph-theoretic models for pipe net-work analysis. *Journal of Hydraulic Division, ASCE*, 98 (2), 345–364.

Isaacs, L.T. and Mills, K.G., 1980. Linear Theory Method for Pipe Network Analysis. *Journal of Hydraulic Division, ASCE*, 106 (7), 1191–1120.

Martin, D.W. and Peters, G., 1963. The application of Newton's method to network analysis by digital computers. *Journal of the Institute of Water Engineer*, (17), 115–129.

Mignosa, P., 1987. Sui problemi di verifica delle reti di distribuzione idrica complesse. *Idrotecnica*, (6), 257–273.

Osiadacz, A.J., 1987. *Simulation and analysis of gas networks*. London: E. and F.N. Spon, London.

Piller, O., 1995. *Modeling the behavior of a network – Hydraulic analysis and a sampling procedure for estimating the parameters*. PhD thesis. University of Bordeaux I.

Rossman, L.A., 2000. *Epanet2 Users Manual*. US EPA.

Shamir, U. and Howard, C.D.D., 1968. Water distribution network analysis. *Journal of Hydraulic Division, ASCE*, 94 (1), 219–234.

Todini, E., 1979. Un metodo del gradiente per la verifica delle reti idrauliche. *Bollettino degli Ingegneri della Toscana*, 11, 11–14 (in Italian).

Todini, E., 1999. *A unifying view on the different looped pipe network analysis algorithms, computing and control for the water industry*. Baldock, UK: Research Studies Press Ltd., 63–80.

Todini, E., 2003. A more realistic approach to the extended period simulation of water distribution networks. *Advances in water supply management*. Balkema Publishers, 173–184.

Todini, E. and Pilati, S., 1988. A gradient method for the solution of looped pipe networks. *Computer applications in water supply*. Vo.1. John Wiley and Sons, 1–20.

Wood, D.J. and Charles, C.O.A., 1972. Hydraulic network analysis using linear theory. *Journal of Hydraulic Division, ASCE*, 98 (7), 1157–1170.

Wood, D.J. and Rayes, A.G., 1981. Reliability of algorithms for pipe network analysis. *Journal of Hydraulic Division, ASCE*, 107 (10), 1145–1161.